Submitted to the International Europhysics Conference on High Energy Physics,
EPS97, Jerusalem, Israel, August 1997

A New Method of Determining the Gluon Density in the Proton from Jet Rates in Deep Inelastic Scattering

H1 Collaboration

Abstract:

A method of determining the proton gluon density in the fractional momentum range $0.01 < \xi < 0.3$ is presented in a next to leading order QCD fit using jet rates in deep inelastic positron proton scattering. This paper discusses the method of Mellin transforms used for performing the fits and demonstrates its viability using data taken with the H1-detector in 1994 and 1995 for an integrated luminosity of $6.5\ \mathrm{pb}^{-1}$.

Abstract 244
Parallel Sessions 2,3,4
Plenary Sessions 1,2,3

1 Introduction

The analysis of deep inelastic positron (electron) proton scattering experiments at HERA has led to new information on the gluon density $f_{g/p}(\xi,\mu^2)$ inside the proton as function of the fractional gluon momentum ξ in the proton infinite momentum frame and the factorization scale μ^2. On one hand the scaling violations of the structure function F_2 measured in the inclusive reaction $e+p\to e+X$ have been analyzed [1] in next to leading order (NLO) QCD, resulting in a determination of the gluon density in the range $2\cdot10^{-4}<\xi<3\cdot10^{-2}$. On the other hand there are final state observables which are sensitive to $f_{g/p}(\xi,\mu^2)$. Take for example the production of two hard jets together with the remnant jet. In leading order QCD this process is described by the generic Feynman diagrams of fig. 1 and the cross section can be written as

$$\frac{d\sigma_{2+1}}{dxdQ^2}\sim\int\frac{d\xi}{\xi}f_{q/p}(\xi,\mu^2)C_C^{LO}(\frac{x}{\xi})+\int\frac{d\xi}{\xi}f_{g/p}(\xi,\mu^2)C_F^{LO}(\frac{x}{\xi}) \tag{1}$$

i.e. a sum of the quark initiated QCD-Compton process and the gluon initiated fusion process with coefficient-functions $C_{C,F}^{LO}$ calculable in QCD [2]. In the equation above, x and Q^2 denote as usual the Bjorken scaling variable and the absolute value of the squared four momentum transfer between the incoming and outgoing positron. It is also customary to identify the factorization scale with Q^2. In LO the fractional momentum ξ can be calculated from the invariant mass $\hat{s}$ of the two hard jets via

$$\xi=x\frac{Q^2+\hat{s}}{Q^2}\quad. \tag{2}$$

This allows for a direct determination of ξ and extraction of $f_{g/p}(\xi,\mu^2)$ from the second integral in eq. (1), provided the quark densities in the first integral are taken from other measurements. An analysis along these lines has been presented earlier by the H1 collaboration [3] resulting in an LO determination of $f_{g/p}(\xi,\mu^2)$ in the range $3\cdot10^{-3}<\xi<10^{-1}$.

An application of this method in second order QCD is highly desirable. In NLO after including virtual and real corrections to the diagrams of fig. 1 the coefficients $C_{C,F}^{LO}(\xi)$ are replaced by $C_{C,F}^{NLO}(\xi,\mu^2)$ but the general structure of eq. (1) remains unchanged. It is however not possible anymore to directly determine ξ from external observables because the coefficients $C_{C,F}^{NLO}$ are now distributions, not regular functions, and thus only defined within the integrals.

An obvious remedy for this problem is to either apply an unfolding procedure yielding $f_{g/p}$ in bins $\Delta\xi_i$ of ξ (with usually different values μ_i^2 in each ξ-bin) or to apply a fitting procedure. The performance of a fit would normally consist of the repeated use of the three step procedure

Figure 1: Generic Feynman diagrams in LO QCD, left hand side : QCD Compton process, right hand side : Boson Gluon Fusion.

- choose an ansatz for $f_{g/p}(\xi, \mu_0^2)$ at a low scale μ_0^2, for example the three parameter polynomial
$$\xi f_{g/p}(\xi, \mu^2) = A_N \xi^\alpha (1 - \xi^\beta)(1 + \gamma\xi) \ , \tag{3}$$
where the normalization constant A_N is fixed by the momentum sum rule.

- select a known parameterization of the quark densities and evolve $f_{g/p}$ to the scale μ^2.

- calculate the integrals in eq. (1) and compare with the measured data.

A closer inspection of this method shows that its application in a typical experimental environment is prohibitive, because it is very consumptive in computer time resources. The calculation of σ_{2+1} including cuts and detector acceptances is usually done numerically and programs like DISENT [4] and MEPJET [5] which include the higher order QCD terms need more than 24 hours on a modern workstation for one set of parameters.

It was therefore proposed [6] to use the method of Mellin-transforms. The Mellin transforms F_n of a function $F(z)$ are defined by $\int_0^1 z^n F(z) dz/z$, and the transforms (or moments) σ_n of the cross section factorize
$$\sigma_n = f_n \, C_n \tag{4}$$
into moments f_n,C_n of the parton density and the coefficient functions (of course separately for the two integrals of equation (1)). The inversion of σ_n yields the cross section σ_{2+1} again. This procedure allows for a fast repeated calculation of σ_{2+1}, since the time consuming determination of C_n can be done once and for all, while the variation of $f_{g/p}$ and subsequent Mellin transform calculation in the fit is very fast. In this paper it will be shown, that the method produces useful results already with the limited amount of data available at present.

The experimental and theoretical determination of jet cross sections requires the choice of a jet algorithm to separate the selected class of (2+1) jet events. In recent years a lot of experience has been gathered for the application of the JADE [7, 8] algorithm in deep inelastic scattering experiments [9, 10]. The use of this formalism introduces a further technical problem. It renders the functions $C_{C,F}$ unfactorizable, i.e. these functions –besides their dependence on x/ξ– depend explicitly on x, which forbids their direct use in the Mellin-method. In ref. [6] a solution to this problem has been given. It consists in a variable transformation at the prize, that a cross section differential in x can only be obtained by subtracting two integrated cross section with different upper limits in x.

Because of the limited statistics of the data only cross sections $d\sigma/dQ^2$ fully integrated over the available x-range are used in this paper. Moreover in order to avoid the problems of absolute cross section measurements, the (2+1) jet-*rates* defined as
$$R_{2+1}(Q^2) = \frac{\sigma_{2+1}}{\sigma_{1+1} + \tilde{\sigma}_{2+1}} \tag{5}$$
are taken as observable for the analysis presented below. Here σ_{2+1} is the cross section for final states with two hard jets in the jet acceptance region of the detector. The denominator is a very good approximation to $\sigma_{\rm tot}$ because the number of events with 3 and more hard jets is negligible. The tilde symbol indicates that all events are included where at least one jet falls in the jet acceptance region.

The data corresponding to an integrated luminosity of 6.5 pb^{-1} are discussed in detail in ref. [11], where they are applied for the determination of the strong coupling constant $\alpha_s(Q^2)$ assuming a given set of parton densities $f_{q/p}$ and $f_{g/p}$. In this paper, the alternative point of view is exploited: the strong coupling constant is taken from the global fits of the parton density functions and the data are used to determine $f_{g/p}$.

The y_{cut}-parameter of the JADE-algorithm needed for the separation of the jet-classes [7] was set to 0.02 in ref. [11]. This in turn implies that ξ as defined in the LO-relation (2) is bigger than 0.02 [9]. Because of the strong decrease of the cross section with ξ there is a close correlation of the jet rates $R_{2+1}(Q^2)$ with the gluon density at $\xi = 0.02$.

2 Tools

The H1 Detector Deep inelastic $e\,p$ scattering events were collected with the H1 detector at HERA ($E_e = 27.5$ GeV, $E_p = 820$ GeV, $\sqrt{s} = 300$ GeV). The H1 detector is described elsewhere [12]; here only the components relevant for the present analysis are briefly recalled. Only calorimetric information is used to reconstruct electromagnetic and hadronic clusters. The event vertex and the direction of the scattered lepton are obtained with the tracking detectors.

The calorimeter system consists of a liquid argon (LAr) calorimeter, a backward calorimeter and a tail catcher (instrumented iron yoke). The LAr sampling calorimeter covers the polar angle[1] range $4° \leq \theta \leq 153°$ and all azimuthal angles. It consists of a lead/argon electromagnetic section followed by a stainless steel/argon section for the measurement of hadronic energy. Electromagnetic energies are measured with a resolution of $\sigma(E)/E \simeq 12\%/\sqrt{E} \oplus 1\%$ and hadronic energies with $\sigma(E)/E \simeq 50\%/\sqrt{E} \oplus 2\%$, as obtained from test beam results. The absolute energy scales are known to 3% and 4% for electrons and hadrons, respectively. A lead/scintillator electromagnetic backward calorimeter (BEMC) extends the coverage at large angles ($155° \leq \theta \leq 176°$). [2] The electromagnetic energy calibration is known to 1%. The instrumented iron flux return yoke is used to measure the leakage of hadronic showers.

Located inside the calorimeters is a tracking system, which consists of central drift and proportional chambers ($25° \leq \theta \leq 155°$), a forward track detector ($7° \leq \theta \leq 25°$) and backward proportional chambers ($155° \leq \theta \leq 175°$). The tracking chambers and calorimeters are surrounded by a superconducting solenoid coil providing a uniform field of 1.15 T within the tracking volume.

The luminosity is determined from the rate of the Bethe–Heitler process $e\,p \to e\,p\,\gamma$ measured in a luminosity monitor far downstream in the electron direction.

The QCD programs The theoretical calculations needed for the calculation of the cross section cannot be performed analytically, but with the means of a cross-section Monte Carlo. In this paper DISENT is used.

DISENT [4] implements next-to-leading order corrections to (1+1) and (2+1) jet events in DIS. The subtraction method is used to handle the divergent parts of the integration. In addition DISENT does not require the approximation of the $s_{\rm min}$ cut–off introduced in the phase-space slicing method. The event generator like structure of the user data allows phase space cuts, the application of jet algorithms and an interface to calculate the Mellin transforms.

There is another NLO program MEPJET [5], which uses the phase space slicing method and therefore needs crossing functions as input. This technique greatly complicates the calculation of the transforms and hence DISENT is used for all calculations. Comparisons for given particle density functions, however, show a good agreement of both programs.

Fitting the Gluon Density with the Mellin Transform Technique For the purpose of fitting the gluon density, the (2+1) jet cross sections used to calculate the jet rate as defined in eq. (5) are split up into the sum of the gluon and quark induced part. The quark induced contributions can be integrated directly by DISENT, while the gluon induced cross sections are calculated by the Mellin transform method. This involves the computation of one set of transforms per bin in Q^2 for σ_{2+1} to $\mathcal{O}(\alpha_S^2)$ (i.e. NLO) and one set $\tilde{\sigma}_{2+1}$ to $\mathcal{O}(\alpha_S)$ (i.e. LO). In

[1] Polar angles θ are defined with respect to the incident proton direction.

[2] Since 1995 the BEMC and BPC in the backward region have been replaced by a lead/scintillating fibre calorimeter (SPACAL) and a drift chamber (BDC). But in the analysis presented here, for $Q^2 < 100$ GeV^2 data taken in 1994 are used only.

a previous publication [6], it was shown that it is possible to reproduce the cross section to an accuracy of within 1 %, compared to a direct integration.

For each selection of α, β, γ, the transforms of the gluon density $f_{g/p}$ are calculated at the starting scale Q_0^2 and subsequently evolved in Mellin transform space to the desired scale Q^2. The product of $f_n C_n$, as defined in eq. (4), is then inverted to yield the cross section in the desired Q^2 bin. In this paper, $Q_0^2 = 4$ GeV^2 will be used. The sum of the quark and gluon induced cross sections enter the calculation of the jet rate, which can subsequently be compared to data. This is performed by a χ^2 fit. For the actual numerical determination of the χ^2 minimum, the widely used package MINUIT is employed [13]. Special care is required for the error treatment.

In order to determine an error of the fit, the straightforward method of using the MINOS option of [13] is not feasible, since the three parameter fit of jet rates forms a rather complex mathematical problem, and it turns out that the MINOS procedure does not converge, nor does it produce an error estimate. The reason is essentially that, in this case, it is not easily possible to compute error matrices with the parameters varied such that χ^2 is increased by 1 from the location of the local minimum that constitutes the solution of the fit. If the χ^2 function rises by less than 1 before it decreases again in any direction of parameter-space, this procedure does not produce a solution.

To overcome that difficulty, one can use an estimation procedure that uses the parabolic error of the three parameters given by the fit. This error is defined as the change of the parameter necessary to increase χ^2 by 1, for each parameter separately. The difference to the "full" mathematical error treatment lies in the fact that correlations between the parameters are not taken into account. Additionally, it is assumed that χ^2 varies parabolically with the variation of a parameter, hence the expression "parabolic." This can be achieved with the HESSE option in [13]. The parabolic approximation is calculated from finite differences, which implies a dependence of this procedure of the of the χ^2-function around the minimum. The drawback of this method is the necessity to exert extra care in selecting start values and error estimates for the fit.

This error estimate is an upper bound to the error by MINOS, and can therefore be taken as a measure. It produces an error band around the fit value for any given scale Q^2 in the ξ range under consideration by taking all permutations of $\alpha \pm \Delta\alpha$, $\beta \pm \Delta\beta$, and $\gamma \pm \Delta\gamma$ at Q_0^2, evolving to the scale Q^2 and taking the spread as the error.

In order to demonstrate the applicability of this procedure, (2+1) jet rates defined by MRSD-' [14, 15] were calculated with the cuts similar to the ones described in section 3. An overall error of 5% was assumed for these test data. The result is shown in fig. 2. It shows nicely that the central value of the fit is well reproduced and the error band is narrow in the region where the fit is sensitive and widens up for lower ξ in the extrapolated region, as expected (see introduction). Further details can be found in [16].

3 Data Selection Procedure

Data Selection The data used here has been studied as part of an analysis measuring the strong coupling constant α_s. Details of the event selection can be found in [11].

The events are divided into two subsamples corresponding to the detector component the scattered electron is found in. For an event $Q^2 < 100$ GeV^2 the lepton is scattered into the backward electromagnetic calorimeter (BEMC). As this detector was replaced in 1995, data of the 1994 data taking period is used. In the high Q^2 sample the liquid argon calorimeter (LAr) contains the scattered electron hits. In this region 1994 and 1995 data are taken into account.

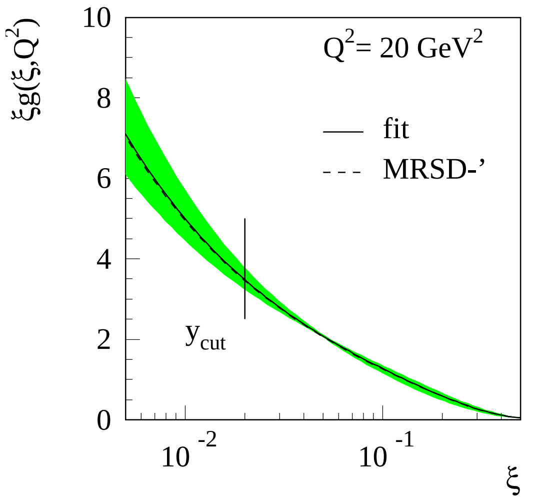

Figure 2: Comparison of parametrized gluon density from known R_{2+1} with MRSD-' by introducing a $\sim 5\%$ error into the fit, which resulted in the shaded area.

Scattered electron found in	BEMC	LAr
Q^2	$40\ \mathrm{GeV}^2 - 100\ \mathrm{GeV}^2$	$100\ \mathrm{GeV}^2 - 4000\ \mathrm{GeV}^2$
minimal scattered electron energy E'_e	14 GeV	11 GeV
scattered electron angle θ'_e	$160°...173°$	$10°...150°$
$y_{\max}$	no cut	0.7
$\sum_{\text{clusters}} E - P_z$	no cut	38 GeV...70 GeV
Vertex position z_{vertex}	$1994:\ 5\ \mathrm{cm} \pm 30\ \mathrm{cm}$	
	$1995:\ 1\ \mathrm{cm} \pm 30\ \mathrm{cm}$	
minimal invariant hadronic mass W^2	$5000\ \mathrm{GeV}^2$	

Table 1: Event selection cuts.

Table 1 summarizes the selection criteria for both samples.

After the basic event selection a modified JADE algorithm [7, 8] is applied in the laboratory frame, using the squared invariant hadronic mass W^2 as scale and a cut value of $y_{\text{cut}}= 0.02$.

Depending on the number of current jets, additional cuts are tested :

- For each event the polar angle of at least one current jet has to be in the range $10° < \theta_{\text{jet}} < 145°$.
- For the 2+1 events both current jets have to lie inside the range given above and the $z_p = \frac{1}{2}(1 - \cos\theta^*_{\text{jet}}) = \frac{E_{\text{jet},i}(1-\cos\theta_{\text{jet},i})}{\sum_{j=1}^{2} E_{\text{jet},j}(1-\cos\theta_{\text{jet},j})}$ value has to be greater than 0.1, where θ^*_{jet} is the smaller of the angles of the two jets in the photon-parton center of mass system.

These requirements define two event classes. Events passing the first condition are counted for the total number of events N_{sample} and those fulfilling the second one in addition are also treated as (2+1) jet events N_{2+1}.

The jet rate defined in eq. (5) is then calculated as

$$R_{2+1} = \frac{N_{2+1}}{N_{\text{sample}}} \tag{6}$$

	Q^2/ GeV^2 Bin			
	40 – 100	100 – 300	300 – 700	700 – 4000
Jetrate	*0.0472*	*0.0683*	*0.0868*	*0.1079*
Statistics	**0.0057**	**0.0045**	**0.0064**	**0.0113**
θ_{jet} **and** z_p	**0.0057**	0.0035	**0.0052**	**0.0121**
Hadronic Energy Scale	0.0038	**0.0052**	0.0044	0.0075
Parton Shower and Hadronization Param.	0.0041	0.0078	0.0049	0.0046
Monte Carlo Model	0.0063	0.0037	0.0099	0.0114
μ_f^2, μ_r^2 **Scale**	**0.0089**	**0.0125**	**0.0107**	**0.0122**
α_s	0.0048	0.0057	0.0057	0.0053
total error	0.0120	0.0143	0.0135	0.0206

Table 2: Uncertainty in jet rate for all Q^2 bins. Errors are devided into three classes : statistics, experimental systematics and theoretical. The dominant source in each class is printed in bold. For details see text. Values partly from [11].

To compare data with QCD NLO theory the data has been corrected for detector and hadronization effects. This is done using the Lepto Monte Carlo [17].

This procedure is performed in four Q^2 bins ranging from 40 GeV^2 up to 4000 GeV^2. Table 2 shows the corrected jet rate, values are taken from [11].

Error Calculation In addition to the statistical error experimental and theoretical uncertainties are calculated. See table 2 for the full list.

To determine the experimental error two scenarios are taken into account :

- A priori the gluon density is independent of any phase space variations, but the systematic error analysis in [11] shows a small variation of the strong coupling constant w.r.t. different jet cuts. Therefore a scheme is defined to estimate the uncertainty in the jet rate.

  The jet rate of the corrected data R^d_{2+1} and of the theory prediction R^t_{2+1} is calculated for the central cut values (CV) and additional scenarios. The systematic uncertainty is then determined by :

  $$\Delta R = \max_{\text{scenarios}} \left| R^d_{2+1} - R^d_{2+1}(CV) - (R^t_{2+1} - R^t_{2+1}(CV)) \right|$$

  Firstly, one jet cut is varied, leaving the other parameters at their central values. The values[3] used for each parameter are :

  - $z_p > 0.05, \mathbf{0.1}, 0.15$
  - $\theta_{\text{jet}} > 0°, 5°, 8°, \mathbf{10°}, 12°, 15°$
  - $\theta_{\text{jet}} < 140°, \mathbf{145°}, 150°$

  In addition the combinations $z_p > 0.15, 5° < \theta_{\text{jet}} < 145°$ and $z_p > 0.05, 15° < \theta_{\text{jet}} < 145°$ are used.

- The hadronic energy scale in the data reconstruction is varied by $\pm 4\%$.

[3]central values are displayed in bold.

For the theoretical error several uncertainties were investigated :

- To estimate the uncertainty in the Monte Carlo correction procedure several parton shower and hadronization parameters in JETSET [18] are varied :
  - the fragmentation parameters a and b of the LUND fragmentation functions are varied between 0.1 and 1,
  - the σ_{pt} parameter and the intrinsic k_T of the struck parton are varied between 0.44 and 0.7,
  - the lower cut-off parameters which control the parton shower generation are varied between 1 GeV and 4 GeV,
  - the lowest invariant mass squared $\hat{s}$ of the two generated partons for which the matrix element calculations are carried out is changed from 4 GeV^2 to 25 GeV^2,
  - the Gaussian width of the primordial p_x and p_y in the jets is varied between 0.25 GeV and 0.45 GeV.
- The dependence of the correction to the partonic level on the Monte Carlo Model is estimated by using HERWIG [19] instead of the standard LEPTO program.
- The $\Lambda^{(5)}_{\overline{MS}}$ value is varied in the range of 0.169 GeV to 0.296 GeV around its central values of 0.226 GeV corresponding to an $\alpha_s(M_Z^2)$ of 0.118 ± 0.005.
- Changing the factorization and renormalization scale independently between $Q^2/4$ and $4Q^2$ is used as a measure of the scale dependence. This turns out to be the main contribution of the theoretical uncertainty.

Following the procedure in [20] the error in each class is taken as the maximum spread and the total error of the jet rate is then calculated as the quadratic sum. This procedure accounts for possible correlations of the different sources of uncertainty.

4 Results

The performance of a stable three parameter fit for $f_{g/p}(\xi, Q^2)$ from the four measured jet rates $R_{2+1}(Q^2)$ turned out not to be an easy task. The main reason is that the sensitivity of the rates on the gluon density decreases rapidly with increasing Q^2 and that most of the gluon induced events originate from gluons with a momentum fraction close to $\xi = y_{cut}$. The jet rates thus most strongly determine the value of the parameter α in ansatz (3).

In order to constrain the range of β an additional data point at high ξ is needed. Prompt photon production in pp and $p\bar{p}$ collisions at high transverse momenta has been analyzed in [21] in terms of $f_{g/p}$. From this analysis, $f_{g/p}(\xi = 0.2, Q^2 = 20\mathrm{GeV}^2) = 0.550 \pm 0.115$ is added to our data set. A stable fit is then obtained for which $\alpha = -0.465, \beta = 5.6, \gamma = 8.8$ with $\chi^2 = 2.27$ for 2 degrees of freedom. The error on each parameter from this fit does not reflect their uncertainty and is therefore not quoted.

The corresponding gluon density evolved to $Q^2 = 20$ GeV^2 and $Q^2 = 100$ GeV^2 is shown in fig. 3 in the range $0.01 \leq \xi \leq 0.3$. This range is determined by the input from jet data and the prompt photon data and corresponds to the region, where our determination is most sensitive. The band represents the maximum spread allowed by the error of the parameters in the fit. Note that at $Q^2 = 20$ GeV^2 the fitted gluon density is 0.640 ± 0.004, close to the input value from the prompt photon production analysis. The crossover at $\xi = 0.055$ for $Q^2 = 20$ GeV^2

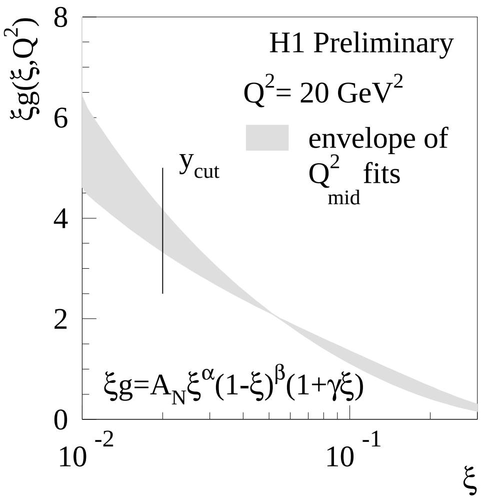

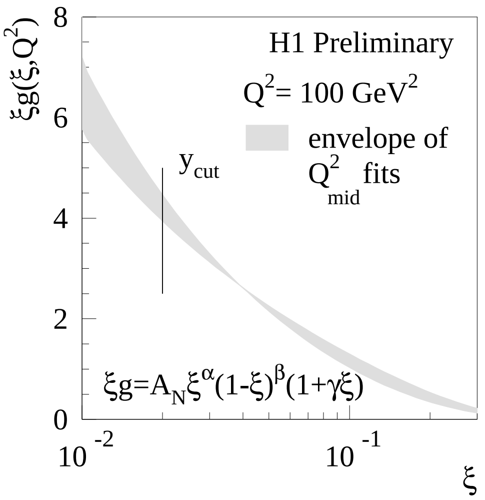

Figure 3: Parametrization of the gluon density obtained from data, plotted for the scale $Q^2 = 20\ \mathrm{GeV}^2$ (left) and $Q^2 = 100\ \mathrm{GeV}^2$ (right).

bin boundaries	Q^2_{mid} set		
$Q^2_{\mathrm{min}} \ldots Q^2_{\mathrm{max}}[\ \mathrm{GeV}^2]$	$Q^2_{\mathrm{mid}}[\ \mathrm{GeV}^2]$	$Q^2_{\mathrm{low}}[\ \mathrm{GeV}^2]$	$Q^2_{\mathrm{high}}[\ \mathrm{GeV}^2]$
$40 \ldots 100$	63.25	40	100
$100 \ldots 300$	173.21	105	286
$300 \ldots 700$	458.26	300	700
$700 \ldots 4000$	1673.32	1015	2760

Table 3: Q^2 sets used in this analysis. The sets are defined as follows : $Q^2_{\mathrm{mid}} = Q_{\mathrm{min}}Q_{\mathrm{max}}, Q^2_{\mathrm{low}} = \max(Q^2_{\mathrm{min}}, 1.65Q^2_{\mathrm{mid}}), Q^2_{\mathrm{high}} = \min(Q^2_{\mathrm{max}}, Q^2_{\mathrm{mid}}/1.65)$. For more information see text.

and $\xi = 0.035$ for $Q^2 = 100\ \mathrm{GeV}^2$ is an artifact of the ansatz (3) and the strong correlation of the resulting coefficients and the fixed quark densities. These crossover points are a well known feature from other parton density fits (see e.g. [22]). They depend on the ansatz chosen, but replacing ansatz (3) by another popular form, i.e. substituting the linear term $\gamma\xi$ by $\gamma'\sqrt{\xi}$, alone did not lead to a stable fit.

The analysis so far has neglected the fact that the data are summed up in Q^2 bins, whereas the evolution during the fit procedure takes place at a fixed Q^2_{mid} per bin. To be consistent in the calculation, the factorization scale in DISENT has to be set to Q^2_{mid}, too. This introduces an additional uncertainty due to the fact, that the full renormalization group equation is used to evolve the gluon density from Q^2_0 to Q^2_{mid}, but the remaining evolution from Q^2_{mid} to Q^2_{event} is done in an approximation which neglects terms of the order $\alpha_s^n \log^n\left(\frac{Q^2_{\mathrm{mid}}}{Q^2_{\mathrm{event}}}\right)$ [23]. To minimize the effect, $Q^2_{\mathrm{mid}} = Q_{\mathrm{min}}Q_{\mathrm{max}}$ is used, with Q_{min} and Q_{max} being the boundaries of each bin. It was checked, that $\left|\log\left(\frac{Q^2_{\mathrm{mid}}}{Q^2_{\mathrm{event}}}\right)\right| \ll 1$ for all $Q_{\mathrm{min}} < Q_{\mathrm{event}} < Q_{\mathrm{max}}$.

Table 3 shows the resulting Q^2_{mid} values. In addition two extreme sets are defined to get an estimate of the uncertainty introduced. The actual values are defined by the condition $\left|\ln\left(\frac{Q^2_{\mathrm{set}}}{Q^2_{\mathrm{event}}}\right)\right| = 0.5$, unless Q^2_{set} is outside the Q^2 bin, in which case the bin boundary is taken.

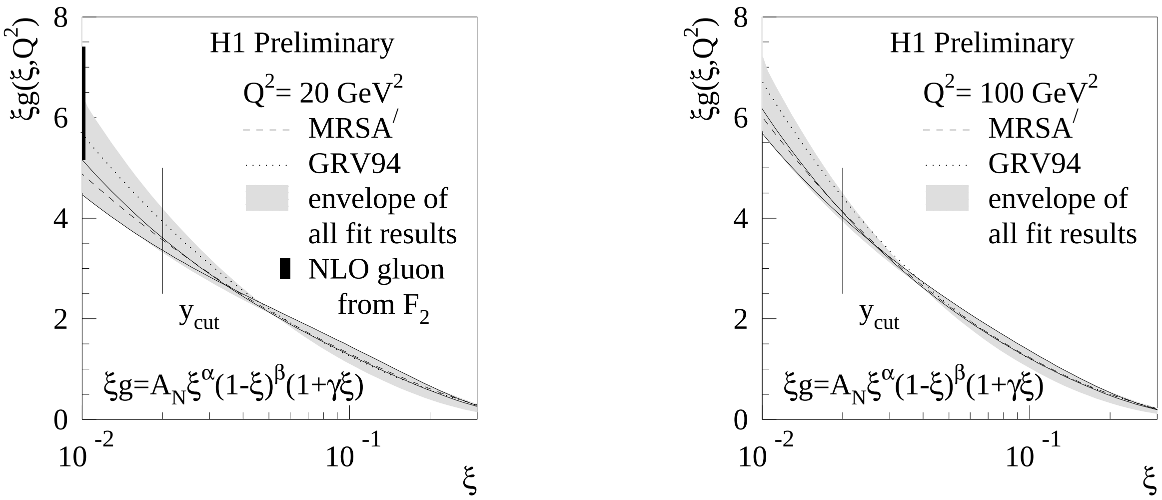

Figure 4: Fit of the parametrized gluon density obtained from data for the three different $Q^2_{\rm mid}$ sets as described in the text. Plotted for the scale $Q^2 = 20$ GeV^2 (left) and $Q^2 = 100$ GeV^2 (right). The shaded band denotes the envelope of all gluon densities allowed by the errors of the fit coefficients. Also included are two typical results (thin lines) and the predictions of the MRSA' (dashed curve) and GRV94 (dotted curve) parameterization. The dark bar on the left hand boundary of the left figure represents the new H1 result obtained from a fit of the scaling violations of the structure function [24].

The gluon densities for the three sets are overlayed in fig. 4. All curves are consistent with each other. Two thin lines show two typical fit results for ansatz eq. (3). The shaded band represents the envelope of all fit results including the uncertainty in each of the fitted parameters in ansatz eq. (3).

The above procedure can be translated into an estimate of the uncertainties of the parameters, which correspond to the envelope of all fit results, as follows. The central value is taken to be the parameter value for the fit using $Q^2_{\rm mid}$. The uncertainty is taken to be the maximum difference possible between the parameter value using $Q^2_{\rm mid}$ and its value at $Q^2_{\rm low}$ or $Q^2_{\rm high}$, including also the uncertainty of the latter. This yields :

$$\begin{aligned}\alpha &= -0.465 \pm 0.010\\ \beta &= 5.6 \pm 1.0\\ \gamma &= 8.8 \pm 6.8\end{aligned} \tag{7}$$

Evolving the gluon density to $Q^2 = 30$ GeV^2 shows good agreement with the direct LO determination performed in a previous publication [3]. It also extrapolates smoothly to the fitted gluon density at smaller ξ values obtained in the H1 analysis of the scaling violations [24] of the structure function F_2. The fit result is also compared to the GRV and MRSA' NLO parameterization in fig. 4. The agreement is very good, demonstrating that NLO QCD provides a consistent description of both F_2 evolution and (2+1) jet production in deep inelastic scattering.

As explained in the introduction the method assumes, that the quark densities are known. For the fits presented in this paper they have been taken from the MRSH parameterization [25]. The influence of other quark densities will be tested when data with higher statistics over a wider range of the kinematical variables are analyzed for a more precise determination of $f_{g/p}$ at values of $\xi > 0.01$.

5 Conclusions

A new method of determining the proton gluon density in next to leading order QCD has been applied. The approach uses jet rates as the experimental observable and the method of Mellin transforms. Using data taken with the H1 detector in 1994 and 1995 and assuming a plausible parametrization of the fractional momentum dependence ξ, results are obtained which are consistent with next to leading order QCD fits to the proton structure function F_2 evolution. Before a full error calculation can be made for such a determination of the proton gluon density from (2+1) jet rates in next to leading order QCD, more data are needed.

Acknowledgments We are grateful to the HERA machine group whose outstanding efforts have made and continue to make this experiment possible. We thank the engineers and technicians for their work in constructing and now maintaining the H1 detector, our funding agencies for financial support, the DESY technical staff for continual assistance, and the DESY directorate for the hospitality which they extend to the non–DESY members of the collaboration. We gratefully acknowledge valuable discussions with D. Graudenz, M. Seymour, and A. Vogt.

References

[1] H1 Collaboration, S. Aid et al.; Phys. Lett. B354 (1995) 494-505, hep-ex/9506001.

[2] A. Mendez, Nucl. Phys. B145 (1978) 199;
R.D. Peccei, R. Rückl, Nucl. Phys. B162 (1980) 125.

[3] H1 Collaboration, S. Aid et al.; Nucl. Phys. B449 (1995) 3-24, hep-ex/9505014.

[4] S. Catani and M.H. Seymour; CERN-TH-96-029, Nucl. Phys. B485 (1997) 291-419, hep-ph/9605323.

[5] E. Mirkes and D. Zeppenfeld; Phys. Lett. B380 (1996) 205, hep-ph/9511448.

[6] D. Graudenz, M. Hampel, A. Vogt, Ch. Berger, Z. Phys. C70 (1996) 77, hep-ph/9506333.

[7] JADE Collaboration, W. Bartel et al., Z. Phys. C33 (1986) 23.

[8] D. Graudenz, N. Magnussen, in: Proc. Workshop "Physics at HERA," DESY, Hamburg, 1991.

[9] H1 collaboration, Phys. Lett. B346 (1995) 415-425.

[10] H1 Collaboration, I. Abt et al.; Z. Phys. C61 (1994) 59-66.

[11] H1 Collaboration; *Determination of α_S from Jet Rates in Deep–Inelastic Scattering;* paper submitted to the International EPS Conference, Jerusalem, August 1997

[12] H1 Collaboration, I. Abt et al.; Nucl. Instr. and Meth. A386 (1997) 310-347 and
Nucl. Instr. and Meth. A386 (1997) 348-396.

[13] F. James, Minuit Program Manual, CERN Program Library Long Writeup D506, Version 94.1.

[14] A.D. Martin, R.G. Roberts, W.J. Stirling, Phys. Rev. D47 (1993) 867-882.

[15] A.D. Martin, R.G. Roberts, W.J. Stirling, Phys. Lett. B306 (1993) 145150,1993, Erratum-ibid. B309 (1993) 492.

[16] M. Hampel, Ph.D. thesis, PITHA 97/13, Aachen, 1997.

[17] G. Ingelman, LEPTO version 6.5, unpublished program manual; see also: LEPTO 6.1, Proc. Workshop “Physics at HERA,” DESY, Hamburg, Vol. 3 (1991) 1366.

[18] T. Sjöstrand, PYTHIA 5.7 and JETSET 7.4, CERN-TH.7112/93;
T. Sjöstrand, Comp. Phys. Comm. 82 (1994) 74-90.

[19] G. Marchesini et al., Comp. Phys. Comm. 67 (1992) 465-508.

[20] ZEUS Collaboration, M. Derrick et al.; Phys. Lett. B363 (1995), 201-216, hep-ex/9510001.

[21] W. Vogelsang, A. Vogt, Nucl. Phys. B453 (1995) 334-354,1995, hep-ph/9505404.

[22] A.D. Martin, R.G. Roberts, W.J. Stirling, Phys. Rev. D43 (1991) 3648-3656.

[23] M.H. Seymour, private communication.

[24] H1 Collaboration, *A Measurement of the Inclusive Deep Inelastic ep Scattering Cross Section at low Q^2 at HERA,* paper submitted to the International EPS Conference, Jerusalem, August 1997

[25] A. D. Martin and W. J. Stirling and R. G. Roberts, MRS parton distributions, Talk given at Leipzig Workshop on Quantum Field Theory Theoretical Aspects of High Energy Physics, Bad Frankenhausen, Germany, 20-24 Sep 1993 and at Topical Meeting on QCD at HERA, Durham, Eng., Mar 22-26, 1993